

Biochemical modelling of microbial memory effects and catabolite repression on soil organic carbon compounds

Daniele la Cecilia^{a,*}, William J. Riley^b, Federico Maggi^a

^aLaboratory for Environmental Engineering, School of Civil Engineering, The University of Sydney, Bld. J05, 2006 Sydney, NSW, Australia.

^bEarth and Environmental Sciences Area, Lawrence Berkeley National Laboratory, Berkeley, CA, 94720, United States

Abstract

1 Microbial decomposition of Soil Organic Matter (SOM) is largely controlled by environmental and
2 edaphic factors such as temperature, pH, and moisture. However, microbial metabolism is controlled by
3 catabolite repression, which leads microbes to grow on preferred nutrient and energy sources first. In par-
4 ticular, Catabolite Repression for Carbon (CR-C) defines the hierarchical preference of bacteria for par-
5 ticular C sources. This control depends on the presence of signal molecules conferring bacteria a memory
6 for recent growth conditions on less preferred C sources. The combined effect of catabolite repression
7 and microbial memory (called here Memory-Associated Catabolite Repression for Carbon, MACR-C)
8 has not yet been investigated in detail. First, we use observations and a numerical model to test the
9 hypothesis that MACR-C explains substrate preferential consumption in a simple, two-C substrate sys-
10 tem, whereas Michaelis-Menten-Monod kinetics of competitive substrate consumption, non-competitive
11 inhibition, or their combination, do not. Next, we carry out numerical analyses to explore the sensi-
12 tivity of (1) estimated parameters to experimental observations and (2) model structure to steady-state
13 substrate concentration under pulse or continuous substrate application. Our results show that MACR-C
14 substantially affected substrate consumption and microbial readiness to switch between C sources.

Keywords:

Diauxic Growth, Catabolite Repression, Substrate Preferential Consumption,
Michaelis-Menten-Monod, Carbon, Soil Organic Matter

1. Introduction

16 Long-term prediction of Soil Organic Matter (SOM) dynamics is crucial to assess soil fertility, envi-
17 ronmental quality, and climate change. Nutrients are continuously added, transformed, and decomposed
18 in soil (Jobbágy & Jackson, 2000) and SOM contains, as a consequence, many different organic com-
19 pounds. Decomposition and bioavailability of SOM are controlled by climate, edaphic conditions, and
20 biogeochemical processes (Doetterl *et al.*, 2015; Dungait *et al.*, 2012). Eventually, accessible substrates
21 are used by microorganisms for their metabolism, and are immobilized in biomass, respired into CO₂,

*Corresponding author.

Email address: daniele.lacecilia@sydney.edu.au (Daniele la Cecilia)

22 or used to synthesize signal molecules, exoenzymes, and exopolymeric substances (Heemsbergen *et al.*,
23 2004; Gunina & Kuzyakov, 2015; Taga & Bassler, 2003; von Bodman *et al.*, 2008; Wardle *et al.*, 2004).

24 Theoretical and numerical frameworks exist to predict the dynamics of carbon- (C) and nitrogen-
25 (N) containing compounds in soil (e.g., Schimel & Weintraub, 2003). However, the variety of chemical
26 compounds in soil is great and they affect the microbial community assembly (Zhalnina *et al.*, 2018)
27 because different bacteria may preferentially consume different substrates. Substrate preferential con-
28 sumption was explained earlier as a result of microbial competition (Fontaine *et al.*, 2003) or substrate
29 consumption inhibition (Wutzler & Reichstein, 2013). Amongst various enzymatic mechanisms, Catabo-
30 lite Repression (CR, Magasanik, 1961) is an alternative hypothesis that has received some attention in
31 complex fermentation systems (Nielsen & Villadsen, 1992; VanDedem & Moo-Young, 1975) but only
32 little attention in the context of SOM cycling. CR regulates the metabolism of various substrates in bac-
33 teria as they continuously fine-tune catabolic and anabolic processes to optimally allocate energy and
34 substrates for cell maintenance or growth. The coordination of these processes has a thermodynamic
35 explanation in the way Gibbs free energy levels in the catabolic and anabolic pathway affect each other
36 (Maggi *et al.*, 2018). CR is therefore presumed to be the result of bacteria adaptation to fluctuating
37 environments; bacteria have a hierarchical preference for beneficial growth substrates and the presence
38 of a preferred substrate may repress gene expression and enzyme activity involved in the metabolism
39 of the non-preferred substrate (Görke & Stülke, 2008; Stülke & Hillen, 1999). The three most relevant
40 mechanisms are global regulation, inducer exclusion, and inducer inhibition. In the first case, the pre-
41 ferred substrate inhibits the expression of the gene(s) involved in the production of the enzyme(s) for the
42 metabolism of the non-preferred substrate; in the second case, the molecule responsible for activating
43 gene(s) expression is prevented from entering the cell, and therefore, from carrying out its task; in the
44 third case, a specific molecule either inhibits gene(s) expression or interferes with enzyme activity. The
45 latter case corresponds to the known mechanisms of competitive consumption, uncompetitive consump-
46 tion, and non-competitive inhibition.

47 Microorganisms that benefit from CR can grow very well on a limited number of substrates, and have
48 evolved mechanisms to hierarchically consume other substrates within mixtures of carbon (Stülke &
49 Hillen, 1999), nitrogen (Farrell *et al.*, 2011), or phosphorus (Wanner, 1993). The most famous example
50 of carbon CR (CR-C) regards *Escherichia coli* growth on a glucose-lactose mixture first observed by
51 Monod (1942), who referred to it as "diauxie", meaning two lagged growth phases each relative to one
52 C source. Later laboratory experiments showed a similar mechanism (Dijkhuizen *et al.*, 1980; Monod,
53 1942; Mukherjee & Ghosh, 1987), but it was Magasanik (1961) who clarified that substrate preferential
54 consumption is due to inhibitory processes. We further this concept as follows: CR-C may not only

55 depend on energy considerations (Ekschmitt *et al.*, 2005) but also on cells' evolutionary trajectories
56 (Lambert & Kussell, 2014). In specific, current growth conditions can stimulate a short-term memory in
57 bacteria due to the combination of phenotypic and response memory (Lambert & Kussell, 2014). The
58 persistent exposure to some substrates may eventually trigger the formation of a long-term memory in
59 the form of genetic networks rearrangements (Stock & Zhang, 2012), such as the optimization of existing
60 pathways for C sources degradation. We identify therefore CR and the memory effect as two aspects that
61 have not yet been fully explored in SOM reaction networks and they may lead to substantial contributions
62 to SOM stability over short and large time scales.

63 We hypothesize that the combined effect of memory and CR, called here Memory-Associated CR
64 (MACR), contributes to control SOM stocks and turnover rates according to both specific substrate pref-
65 erence and the memory of previously consumed substrates. First, we show that classic MMM kinetics
66 cannot predict the dynamics observed in those experiments. Next, we propose that MACR dynamics can
67 be mechanistically described by means of modified Michaelis-Menten-Monod (MMM) kinetics (Monod,
68 1949; Belser, 1989; Bekins *et al.*, 1998; Maggi & Riley, 2010). In particular, we formulate MACR ki-
69 netics for C (MACR-C) using three CR-C experiments with two C sources retrieved from the literature
70 (Dijkhuizen *et al.*, 1980; Mukherjee & Ghosh, 1987). An approach to develop a coupled mechanistic
71 scheme for C and N consumption under MACR was hindered by the lack of suitable laboratory ex-
72 periments. The schemes were assessed by means of visual inspection and error measures. Finally, we
73 performed a suite of sensitivity analyses to assess the long-term effect of MACR-C to pulse and contin-
74 uous C applications into the two 2 C-source systems.

75 **2. Methods**

76 *2.1. Biomass-based and enzyme-based MMM kinetics*

77 Seven schemes of microbial growth on multiple substrates obtained using classic MMM kinetics
78 are shown in Figure 1 together with their MMM kinetic equations. The MMM framework requires the
79 estimation of 3 parameters to predict the consumption rate of a substrate with concentration S (M) as
80 a function of the microbial biomass concentration B (mg L^{-1}). These MMM kinetic parameters are:
81 the reaction rate constant μ (s^{-1}), the half-saturation concentration constant K (M), and the biomass
82 yield coefficient Y ($\text{mg-wet-Biomass mol-C-Substrate}^{-1}$). The terms $(1 + S_P/K_P)$ and $(1 + S_{NP}/K_{NP})$,
83 where subscripts P and NP indicate the preferred and non-preferred substrate, respectively, account for
84 competitive consumption (dashed black lines in Figure 1), which increases K and reduces the reaction
85 velocity. The terms $[K_{I,P}/(S_P + K_{I,P})]$ and $[K_{I,NP}/(S_{NP} + K_{I,NP})]$, where $K_{I,P}$ (M) and $K_{I,NP}$ (M) are
86 the inhibition constants relative to the preferred and non-preferred substrate, respectively, account for

87 inhibition (solid red lines in Figure 1) and also reduce the reaction velocity.

88 Generally, biogeochemical models predict biochemical reactions as a function of microbial biomass.
89 Here, we develop and test both biomass- and enzyme-based frameworks to explicitly account for cells
90 and intracellular enzyme dynamics. The Enzyme (E) (with E in mg L^{-1}) is synthesized by B at rate r_E (L
91 $\text{mol}^{-1} \text{s}^{-1}$) depending on the corresponding substrate availability (i.e., inductive enzymes), and degrades
92 at a rate $\delta_E = \delta$, with δ (s^{-1}) the bacteria mortality rate; δ_E and δ are generally different (Schimel *et al.*,
93 2017) but were assumed here to be the same for simplicity. Enzyme production was inhibited by E with
94 parameter $K_{I,E}$ (mg L^{-1}) assumed equal to 1% of the maximum biomass concentration reached in the
95 experiments.

96 We investigated whether classic MMM kinetics can be used to adequately replicate CR-C observa-
97 tions both in the biomass-based and enzyme-based frameworks. For the latter case, it was tested if CR-C
98 affected substrate catalysis (Figures 1d, e, and f) or enzyme production (Figure 1g).

99 2.2. MACR-C kinetics

100 The schemes in Section 2 were further developed into MACR-C kinetics to take into account the
101 production of a memory signal following substrate consumption, which represents the memory of previ-
102 ous growth conditions and presumably affects CR-C dynamics (Figure 2). To this end, we assumed that
103 the memory signals M_P relative to S_P consumption inhibited S_{NP} consumption, and vice versa for M_{NP}
104 relative to S_{NP} and S_P . MACR-C kinetics were tested in both biomass- and enzyme-based frameworks
105 (Figures 2a and b, respectively). M_P and M_{NP} were assumed to be produced stoichiometrically with S_P
106 and S_{NP} , and degraded according to a first-order reaction with rate δ_M (s^{-1}). E_P and E_{NP} production
107 was assumed to undergo an additional inhibition by M_P and M_{NP} , respectively, with constants K_{I,M_P} and
108 $K_{I,M_{NP}}$.

109 2.3. Experimental data of 2 C-source systems

110 Experimental observations of CR-C in an acetate (ACT) and oxalate (OXL) mixture with *Pseu-*
111 *domonas oxalaticus* OX1, and in a succinate (SCC) and fructose (FRC) mixture with *Azospirillum*
112 *brasilense* were retrieved from Dijkhuizen *et al.* (1980) and Mukherjee & Ghosh (1987), respectively.

113 In the first experiment, ACT and OXL were the only C sources consumed in aerobic conditions.
114 *Azospirillum brasilense* inoculum was pregrown either in ACT or OXL before incubation in two different
115 experiments. *Pseudomonas oxalaticus* OX1 can grow on both ACT and OXL, but prefers ACT.

116 In the second experiment, SCC and FRC were the only C sources consumed in aerobic conditions.
117 *Azospirillum brasilense* can grow on both SCC and FRC, but prefers SCC.

118 Those experiments are interesting because substrates were consumed hierarchically and because they
119 allowed us to test the memory-effect on the microbial CR-C hypothesis.

120 2.4. Method of parameter estimation

121 The unknown parameters μ , K , K_I , K_{IM} , r_E , and δ_M were estimated by inverse numerical solution
122 calculated with the BRTSim solver (based on Maggi, 2015) in the PEST environment (Doherty *et al.*,
123 2016) against experiments from Dijkhuizen *et al.* (1980) and Mukherjee & Ghosh (1987). The biomass
124 yields $Y = \Delta B / \Delta S$ were calculated from observed changes in concentrations of biomass ΔB and substrate
125 ΔS . Cell mortality and enzyme degradation $\delta = \delta_E = 10^{-6} (s^{-1})$ were assumed after Gastrin *et al.* (1968)
126 and Salem *et al.* (2006). O_2 concentration was assumed not to limit the reactions and was not taken into
127 account explicitly. Combinations of competition and inhibition kinetics were tested as per schemes in
128 Figures 1 and 2.

129 Goodness-of-fit was measured with the coefficient of determination $R^2 = [\sigma_{XO} / (\sigma_X \sigma_O)]^2$ and nor-
130 malized root mean squared error percent $NRMSE = \left\{ \sqrt{\frac{\sum_{i=1}^{n_o} (X_i - O_i)^2}{n_o}} / [\max(O) - \min(O)] \right\} \times 100$, where
131 X and O are the modeled and observed concentrations, respectively, and n_o is the number of observations.

132 2.5. Stochastic Sensitivity Analyses on MACR-C parameters

133 In Dijkhuizen *et al.* (1980), the inoculum was pregrown in the non-preferred C-source OXL, and
134 was next grown in the ACT-OXL mixture. In the latter medium, bacteria grew on OXL for a short time
135 before switching to ACT until they depleted ACT, and finally they resumed OXL consumption. To our
136 knowledge, that experiment is the most complete evidence of MACR-C; we conducted stochastic sensi-
137 tivity analyses on this experiment to highlight variability in substrate consumption dynamics using the
138 enzyme-based framework (Figure 2b). In particular, the effects of δ_M , K_{IM} , and r_E on substrate consump-
139 tion were investigated. For each parameter, 1000 simulations were run with values randomly sampled
140 from independent Gaussian probability distributions with mean equal to the corresponding estimated
141 value and standard deviation equal to 20% of the mean.

142 2.6. Steady-state sensitivity analyses on MACR-C dynamics

143 MACR-C kinetics were numerically explored for the two C-source systems using the scheme in
144 Figure 2b with the parameters estimated for the case where the inoculum was pregrown with the corre-
145 sponding preferred C source, ACT and SCC.

146 One analysis elucidated to what extent MACR-C affects the C source concentrations at steady-state
147 given varying continuous incoming C fluxes (e.g., root exudates, SOM cycle, etc...). Each system was
148 continuously amended with S_P and S_{NP} at 0.1 mL s^{-1} flow rate in a 2.5 L control volume containing 1 L

149 of water as solvent (Figure 3a); substrate concentrations ranged from 10^{-7} to 10^{-3} M s^{-1} for ACT, from
150 10^{-7} to 1 M s^{-1} for OXL, from 10^{-7} to 10^{-2} M s^{-1} for SCC, and from 10^{-7} to 1 M s^{-1} for FRC. Excess
151 water was extracted from the control volume at the same flow rate to keep the water volume constant.
152 Ten increments were used within each order of magnitude in concentration.

153 The other analysis elucidated MACR-C effects on the short-term microbial response to sudden pulses
154 of C substrates (e.g. leaching, etc...). MACR-C kinetics were tested for the two C-source systems subject
155 to a single pulse of S_P and S_{NP} lasting 15 s at 0.1 mL s^{-1} flow rate in a 2.5 L control volume containing 1
156 L of water as solvent (Figure 3b). S_P amendment was varied in concentration and was time-shifted with
157 respect to S_{NP} . OXL concentration was 10^{-3} M s^{-1} , while ACT concentration ranged between 10^{-4} and
158 10^{-2} M s^{-1} . FRC concentration was 1 M s^{-1} , while ACT concentration ranged between 0.1 and 10 M
159 s^{-1} . Forty-five increments were used within each order of magnitude in concentration. The system was
160 amended with S_P at times ranging from 1 to 40 days using an incremental step of 4 hours, while S_{NP} was
161 amended at day 10. The S_{NP} degradation times in the presence of S_P were compared to that resulting
162 from S_{NP} consumption alone, that is, S_P was not amended in the system. The time necessary to decrease
163 one substrate concentration below 1% of the initial concentration will be denoted $t_{99\%}$.

164 Our analyses can provide mechanistic information relative to the consumption of chemically similar
165 and different nutrients within a mixture (e.g., ACT-OXL and SCC-FRC carbon-source systems).

166 3. Results

167 3.1. Biomass- and enzyme-based MMM kinetics

168 Classic biomass-based MMM kinetics accounting for substrate competitive consumption, non-competitive
169 inhibition, and their combination, did not capture the observed lag phase when bacteria switched between
170 the two C sources, which is characteristic of CR-C (Figures 4a, b, and c for ACT-OXL mixture and Fig-
171 ures 4d, e, and f for SCC-FRC mixture, goodness-of-fit in Table 1).

172 Classic enzyme-based MMM kinetics did not accurately describe observed CR-C either (Figure 5a
173 to g), except when inhibition of enzyme production was accounted for in the SCC-FRC mixture (Figure
174 5h, goodness-of-fit in Table 1). However, FRC consumption appeared to be slightly anticipated, with an
175 overall rate slower than observed.

176 Despite the additional description of enzyme production and degradation (Figures 1d, e, f, and g),
177 our results suggest that one or more additional processes had substantial effects but were not represented
178 by the tested MMM kinetics.

179 3.2. Biomass- and enzyme-based MACR-C kinetics

180 The MACR-C schemes in Figure 2 replicated the observations when using both biomass- and enzyme-
181 based kinetics (Figure 6, goodness-of-fit in Table 1). Accounting for substrate competitive consumption
182 in MACR-C did not improve the fitting against observations (result not shown) and added an unnecessary
183 parameter; therefore, this mechanism was not accounted for in MACR-C kinetics.

184 The parameters μ , K , r_E , and $K_{I,M}$ estimated after pregrowing the inoculum in ACT captured CR-C
185 also after pregrowing the inoculum with the non-preferred C-source OXL in the enzyme-based frame-
186 work, but not in the biomass-based framework (Table 1). Note that pregrowing bacteria on OXL rather
187 than ACT resulted in lower Y and δ_M . The initial concentrations of enzymes and memory signals were
188 calibrated because they must have been produced during previous growth conditions. Indeed, bacteria
189 started consuming OXL thanks to the memory M_{NP} of pregrowth conditions (Figure 7), but they sensed
190 ACT availability and switched to ACT within approximately 2.4 hours. OXL consumption was therefore
191 repressed in the presence of ACT, and was resumed only after ACT was depleted. Note that none of
192 the schemes in Figure 1 captured these dynamics (results not shown) because the corresponding kinetic
193 equations do not explicitly account for the memory of previous growth conditions that allow microbes to
194 consume part of the non-preferred substrate in the presence of the preferred substrate.

195 MACR-C kinetics captured CR-C dynamics both in the biomass- and the enzyme-based frameworks,
196 and can be considered a robust representation of how memory of previous growth conditions can affect
197 substrate consumption.

198 3.3. Stochastic Sensitivity Analyses on ACT-OXL mixture

199 Stochastic sensitivity analyses on all enzyme-based MACR-C kinetic parameters (i.e., δ_M , $K_{I,M}$, and
200 r_E) showed large variability in ACT and OXL consumption at any time after switching between C sources
201 (Figure 8). The inhibition constant $K_{I,M}$ returned the largest variability in MACR-C response.

202 3.4. Steady-state sensitivity analysis on MACR-C dynamics

203 The steady-state response of the ACT and OXL and the SCC and FRC carbon-source systems to
204 continuous substrate application at varying concentrations were different and highly nonlinear. Gener-
205 ally, the preferred C source concentration (ACT and SCC in Figures 9a and b, respectively) was always
206 negligible and decreased under increased concentrations of the amended substrates. In contrast, the non-
207 preferred OXL substrate concentration (Figure 9a) quickly built up at high ACT and OXL application
208 concentrations. The non-preferred FRC substrate concentration (Figure 9b) also increased at increasing
209 concentrations of amended FRC for $[SCC] > 0.001$ M, but drastically decreased for $[SCC] < 0.001$ M.

210 The two systems responded differently and nonlinearly to single C source pulses at varying concen-
211 trations and time-shifted between each other (Figures 9c and d). OXL (S_{NP}) consumption was slow in
212 the lack of ACT (S_P); OXL concentration took nearly 17.5 days to decrease below 1% of the initial value.
213 ACT pulses did not substantially affect OXL kinetics; early and late S_P pulses lengthened and shortened
214 S_{NP} consumption time by 10% (Figure 9c).

215 FRC (S_{NP}) consumption occurred in nearly 7 days in the lack of SCC (S_P). SCC pulses shortened
216 the time necessary to decrease FRC concentration below 1% of the initial concentration; MACR-C effect
217 was unexpectedly strong with S_P pulses shortening S_{NP} consumption time by up to 7 times (Figure 9d).

218 4. Discussion

219 4.1. MMM kinetics and the MACR-C effect

220 MMM kinetics are widely used to model biochemical processes and are being incorporated in biore-
221 active transport models (e.g., TOUGHREACT, Xu *et al.* 2011; MODFLOW-PHT3D, Prommer *et al.*
222 2001; and HYDRUS, Yu & Zheng 2010). However, this work shows that MMM kinetics are not directly
223 applicable to model substrate consumption when regulated through catabolite repression. While a review
224 of modeling approaches to represent catabolite repression was carried out in Kremling *et al.* (2015), we
225 have shown here that CR-C can be adequately described by introducing a memory signal to inhibit sub-
226 strate consumption. As reported by Stock & Zhang (2012), the memory can be a molecule, and it is
227 characterized by production and degradation rates. We found a lower memory degradation rate in the
228 experiment where the inoculum was pregrown on the non-preferred C source (Table 1). We hypothesize
229 this result implies a mechanism through which bacteria are less prone to switch between C sources in
230 fluctuating environments. As suggested in Lambert & Kussell (2014), a memory may also be corre-
231 lated to the availability of a substrate-specific enzyme. Because both biomass-based and enzyme-based
232 frameworks accurately captured bacterial growth dynamics in the ACT-OXL mixture after pregrowth in
233 OXL, our analysis did not reject the idea of enzyme-carried memory, in addition to microbial memory
234 for preferred substrates. Thus, we found need for a model containing additional parameters to test Lam-
235 bert & Kussell (2014)'s suggestion. However, the available experiments were insufficient to address this
236 question because enzyme-associated memory may play a role over longer timescales. Notwithstanding,
237 although it is more "natural" to describe metabolic processes using enzyme-based models for biochemi-
238 cal reactions inside cells, this approach may result in redundant parameters and, importantly, the problem
239 formulation can be implemented in only a few available bioreactive transport models, such as BRTSim
240 and TOUGHREACT.

241 4.2. The biological role of MACR

242 CR is a common bacterial strategy to select the one substrate amongst many which allow optimal
243 growth (Chu & Barnes, 2016); cells process the information in the surrounding environment, and prepare
244 and activate certain metabolic pathways based on some sort of cost-benefit balance and cell requirements
245 (Wang *et al.*, 2015). We assumed those pathways involve inducible enzymes so that bacteria would not
246 be wasting resources to produce enzymes that may seldom be used for an unknown period of time. In the
247 proposed regulatory mechanism, bacteria can still produce any enzyme in sufficient amount to quickly
248 switch from one substrate to another, thus gaining a fitness advantage in fluctuating environments. Yet,
249 the timing for switching between substrates is regulated by antagonist memory signals, which inhibit
250 the consumption of other substrates. A possible explanation for this inhibition is that cells have earlier
251 invested resources to produce the enzymes involved in one pathway, and only under some circumstances
252 would it be convenient to prematurely invest resources to activate a new pathway.

253 Although we have only focused on C, other macronutrients consumption may be regulated through
254 catabolite repression, which was neglected in this work because of the lack of suitable laboratory exper-
255 iments. However, Farrell *et al.* (2011) reported that peptides are preferred over aminoacids as an organic
256 N source; therefore, the Memory-Associated CR for Nitrogen (MACR-N) could exist and should be in-
257 vestigated. Yet, Roca & Olsson (2001) showed that NH_3 repressed NO_3^- in *Pseudomonas fluorescens*
258 DF57 nitrogen metabolism. Cross-talk amongst macronutrient cycles have been underpinned and re-
259 viewed by Santos-Beneit (2015), focusing on how C and N metabolisms are regulated within cells. This
260 metabolic coupling should be accounted for in SOM models. Yet, the different MACR response to con-
261 sumption of chemically similar or different nutrients, as shown here for the two C-source systems, may
262 represent an additional level of uncertainty to the robust prediction of labile SOM cycles. The estimated
263 kinetic parameters for the memory signal degradation rate, the substrate consumption inhibition con-
264 stant, and the enzyme production rate showed large variability between these two cases. The biological
265 explanation can be revealed by analyzing the environments the bacteria inhabit. Soil bacteria evolved
266 to prefer tricarboxylic acid (TCA) intermediates (Mukherjee & Ghosh, 1987). This evolution explains
267 the hierarchies found between SCC and FRC consumption; the hierarchy is corroborated by Iyer *et al.*
268 (2016)'s comprehensive review on SCC mediated catabolite repression of monosaccharides consump-
269 tion. Despite the greater biomass yield on FRC than SCC, the former very likely requires the production
270 of many enzymes to be broken down to pyruvate, which can eventually enter the TCA cycle and be used
271 for energy production. This energetically-costly process may become convenient when benefits are larger
272 than costs, that is, when FRC concentration greatly exceeds SCC concentration. This inhibitory mecha-
273 nism is fully implemented in MACR-C kinetics. We hypothesize that knowledge of bacteria evolutionary

274 trajectories can help identify representative molecules to be encompassed in comprehensive models of
275 SOM dynamics. For instance, Riley *et al.* (2014) divided SOM into 11 groups, where "Organic Acids"
276 could represent the preferred SOM group, especially when it includes TCA molecules. Such an ap-
277 proach would be supported by recent laboratory investigations highlighting soil bacteria preference to
278 101 metabolites released as root exudates (Zhalnina *et al.*, 2018). These authors found that aromatic
279 organic acids were the bacteria preferred substrate, despite a great variability in uptake by bacteria from
280 the exudate mixture was observed. High uptakes were also found for amino acids, sugars, and quaternary
281 amines. The authors also observed that microbial communities could be either positively or negatively
282 affected in response to metabolites availability. The two groups of responders were characterized by
283 different substrate preference and may therefore inhabit different soil niches (Zhalnina *et al.*, 2018). As
284 a consequence, it is possible that MACR-C kinetics coupled with environmental and edaphic conditions
285 can provide a robust predictive tool to niche colonization and substrate consumption.

286 This work focused on elucidating unexplored mechanisms regulating C preference in soil bacteria.
287 Experimental evidence (Zhalnina *et al.*, 2018) and our modeling results both suggest that MACR-C may
288 play a pivotal role in soil C dynamics. However, it cannot be excluded that bacterial strains lacking
289 CR-C regulatory mechanisms will differently consume available substrates (Johnson *et al.*, 2017). Yet,
290 different types of environments might select bacteria exploiting different mechanisms to thrive amongst
291 other competitors. For instance, the enteric bacteria *E. Coli* constitutively produces enzymes involved
292 in glucose metabolism, thus conferring an advantage in an environment where glucose is almost always
293 available in large amounts.

294 4.3. Physiological meaning of MACR-C kinetic parameters

295 The stochastic sensitivity analysis of MACR-C showed that $K_{I,M}$, δ_M , and r_E produced large variabil-
296 ity in substrates concentration over time and control therefore the hierarchy for substrate consumption
297 and the adaptation time to newly available substrates. These regulatory processes can be embedded in
298 bacterial genetic material and constitute bacteria long-term memory (Stock & Zhang, 2012). In contrast,
299 the initial memory signal M_0 and initial enzyme concentration E_0 had a negligible effects on substrate
300 consumption (not shown). We suggest M_0 and E_0 may represent the bacteria short-term memory pro-
301 duced to provide an advantage in the current environmental conditions. These parameters together quan-
302 tify the strategies exploited by microorganisms to express their preference to a substrate and cope with
303 its absence.

304 In this work, enzyme degradation rate δ_E was assumed to be constant and equal to bacteria mortality
305 δ , while some enzymes can last longer within the cell (Lambert & Kussell, 2014). A longer enzyme
306 persistence would enhance bacterial readiness to consume the corresponding substrate over the long-

307 term. Bacteria memory exerted a powerful inhibitory effect on substrate consumption, but degraded 2 to
308 3 orders of magnitude more rapidly than enzymes, thus having major effects in the short term. Despite
309 bacteria having a preference for some substrates, this memory does not hinder their capability to grow
310 on other substrates in case the former are not available.

311 Our simulations were designed to investigate nonlinearities in substrates consumption under MACR-
312 C kinetics, and for continuous amendments with C sources after steady-state and for pulse amendments
313 with C sources. Both scenarios revealed interesting features. The bacterial long-term memory repre-
314 sented by $K_{I,M}$ and δ_M regulated substrate consumption for varying substrate application concentrations,
315 which may be seen as continuous nutrients arrival from a multitude of processes including advection,
316 SOM decomposition, or necromass recycling. Our results showed that bacteria favor consumption of
317 those substrates allowing for the greatest growth based on availability. Next, S_P pulses at varying con-
318 centrations and time-shifted with respect to a S_{NP} pulse simulated the sudden availability of different C
319 sources. Modeling suggested that early and late S_P pulses had small but distinct effects on the consump-
320 tion of chemically similar and different S_{NP} , resulting in longer or shorter consumption times, respec-
321 tively. For chemically different substrates, consumption times were always substantially shorter with S_P
322 pulses. We speculate that although bacteria prefer to use some C sources, they maintain readiness to
323 switch to others when necessary. In contrast, there is no benefit to switch metabolic pathway for chemi-
324 cally similar C sources as these may have similar nutritional properties. We could not directly assess the
325 role of short-term memory on substrate consumption, which would require the bacteria to be exposed
326 to multiple substrates pulse. With new technologies such as microfluidic devices, bacteria adaptation to
327 non-preferred C sources and the contributions of memory in this process can be studied experimentally
328 (Lambert & Kussell, 2014).

329 4.4. MACR-C and exoenzyme regulation

330 The metabolic regulatory processes occurring within the cell are very complex. To reduce this com-
331 plexity so that it is computationally tractable, MACR-C included 2 kinetic equations to model enzyme
332 and memory dynamics for each substrate. Some more complex C sources such as cellulose have to be
333 first extracellularly decomposed to more labile substrates to become bioavailable to microorganisms.
334 Microorganisms can liberate exoenzymes in the soil matrix to decompose SOM. Some theory for the
335 regulatory mechanisms behind exoenzymes production (De Nobili *et al.*, 2001; Schimel & Weintraub,
336 2003) suggest that small amounts of labile substrates signal the presence of SOM; these molecules trig-
337 ger microbial growth and the production of exoenzymes to keep on decomposing fresh SOM until the
338 bioavailable C is enough to balance the expenditure for exoenzymes production. MACR-C, or more
339 generally MACR, may therefore be involved in regulating exoenzyme production depending on the char-

340 acteristics of available SOM, which will be decomposed to preferred and non-preferred substrates.

341 **5. Conclusions**

342 A detailed kinetic model based on intracellular enzyme dynamics integrating bacterial memory for
343 specific substrates was presented to describe memory-associated carbon catabolite repression (MACR-C)
344 in mixtures of 2 carbon (C) sources. Microbial hierarchic C consumption could not be described using
345 classic MMM kinetics. Instead, MACR-C successfully captured substrates consumption dynamics and
346 the lag phase intercurring while microorganisms switched between the 2 C sources. These dynamics were
347 mechanistically described by accounting for memory signals, which induce bacteria to consume their
348 preferred C source first. We showed that integrating MACR-C in the modeling of steady-state substrate
349 concentration can explain the persistence of theoretically rapidly consumable substrates as a trade-off
350 between bacterial preference for specific substrates, and their prior and current availability. MACR-C
351 is an important process for nutrient cycles and it has not been previously used in land biogeochemical
352 models. MACR-C kinetics can easily be integrated in land models, allowing one to explore with a greater
353 detail microbial contributions to nutrient dynamics under different environmental scenarios, including
354 soil management practices and changes in eco-hydrological boundary conditions, soil biogeochemical
355 characteristics, and land use.

356 **6. Acknowledgements**

357 DLC and FM were supported by the Sydney Research Excellence Initiative (SREI 2020) of The
358 University of Sydney. FM was also supported by the Mid Career Research Award of The University of
359 Sydney and by the Sydney Research Accelerator Fellowship (SOAR) by The University of Sydney. WJR
360 was supported by the Director, Office of Science, Office of Biological and Environmental Research of the
361 US Department of Energy under Contract No. DE-AC02-05CH11231 as part of the TES Scientific Focus
362 Area. The authors acknowledge the Sydney Informatics Hub and the University of Sydney HPC service
363 (http://sydney.edu.au/research_support/). The BRTSim solver package can be downloaded
364 at <https://www.dropbox.com/sh/wrfspx9f1dvuspr/AAD5iA9PsteX3ygAJxQDxAy9a?dl=0>. We
365 thank the Editor Prof. Tim Clough and two anonymous Reviewers for their feedbacks and constructive
366 comments, which contributed to improve this work.

367 **References**

368 Bekins, B., Warren, E., & Godsy, E. 1998. A comparison of zero-order, first-order and Monod biotrans-
369 formation models. *Ground Water*, **36**(2), 261–268.

- 370 Belser, L. W. 1989. Population ecology of nitrifying bacteria. *Annual Review of Microbiology*, **33**,
371 309–333.
- 372 Chu, D., & Barnes, D.J. 2016. The lag-phase during diauxic growth is a trade-off between fast adaptation
373 and high growth rate. *Scientific Reports*, **6**(25191).
- 374 De Nobili, M., Contin, M., Mondini, C., & Brookes, P.C. 2001. Soil microbial biomass is triggered into
375 activity by trace amounts of substrate. *Soil Biology and Biochemistry*, **33**, 1163 – 1170.
- 376 Dijkhuizen, L., van der Werf, B., & Harder, W. 1980. Metabolic Regulation in *Pseudomonas oxalaticus*
377 OX1. Diauxic Growth on Mixtures of Oxalate and Formate or Acetate. *Archives of Microbiology*,
378 **124**(2-3), 261–268.
- 379 Doetterl, S., Stevens, A., Six, J., Merckx, R., Van Oost, K., Casanova Pinto, M., Casanova-Katny, A.,
380 Munoz, C., Boudin, M., Zagal Venegas, E., & Boeckx, P. 2015. Soil carbon storage controlled by
381 interactions between geochemistry and climate. *Nature Geoscience*, **8**(10), 780–783.
- 382 Doherty, J., Muffels, C., Rumbaugh, J., & Tonkin, M. 2016. *PEST Model-Independent Parameter Estima-*
383 *tion & Uncertainty Analysis*. <http://www.pesthomepage.org/PEST.php>. accessed 14.04.2016.
- 384 Dungait, J.A.J., Hopkins, D.W., Gregory, A.S., & Whitmore, A.P. 2012. Soil organic matter turnover is
385 governed by accessibility not recalcitrance. *Global Change Biology*, **18**(6), 1781–1796.
- 386 Ekschmitt, K., Liu, M., Vetter, S., Fox, O., & Wolters, V. 2005. Strategies used by soil biota to overcome
387 soil organic matter stability why is dead organic matter left over in the soil? *Geoderma*, **128**(1), 167
388 – 176.
- 389 Farrell, M., Hill, P. W., Wanniarachchi, S. D., Farrar, J., Bardgett, R. D., & Jones, D. L. 2011. Rapid
390 peptide metabolism: A major component of soil nitrogen cycling? *Global Biogeochemical Cycles*,
391 **25**(3).
- 392 Fontaine, S., Mariotti, A., & Abbadie, L. 2003. The priming effect of organic matter: a question of
393 microbial competition? *Soil Biology and Biochemistry*, **35**(6), 837 – 843.
- 394 Gastrin, B., Kallings, L. O., & Marcetic, A. 1968. The survival time for different bacteria in various
395 transport media. *Acta Pathologica Et Microbiologica Scandinavica*, **74**(3), 371–380.
- 396 Görke, B., & Stülke, J. 2008. Carbon catabolite repression in bacteria: many ways to make the most out
397 of nutrients. *Nature Reviews Microbiology*, **6**(8), 613 – 624.

- 398 Gunina, A., & Kuzyakov, Y. 2015. Sugars in soil and sweets for microorganisms: Review of origin,
399 content, composition and fate. *Soil Biology and Biochemistry*, **90**, 87 – 100.
- 400 Heemsbergen, D. A., Berg, M. P., Loreau, M., van Hal, J. R., Faber, J. H., & Verhoef, H. A. 2004.
401 Biodiversity Effects on Soil Processes Explained by Interspecific Functional Dissimilarity. *Science*,
402 **306**(5698), 1019–1020.
- 403 Iyer, B., Rajput, M.S., Jog, R., Joshi, E., Bharwad, K., & Rajkumar, S. 2016. Organic acid mediated
404 repression of sugar utilization in rhizobia. *Microbiological Research*, **192**(Supplement C), 211 – 220.
- 405 Jobbágy, E.G., & Jackson, R.B. 2000. The vertical distribution of soil organic carbon and its relation to
406 climate and vegetation. *Ecological Applications*, **10**(2), 423–436.
- 407 Johnson, C.W., Abraham, P.E., Linger, J.G., Khanna, P., Hettich, R.L., & Beckham, G.T. 2017. Elim-
408 inating a global regulator of carbon catabolite repression enhances the conversion of aromatic lignin
409 monomers to muconate in *Pseudomonas putida* KT2440. *Metabolic Engineering Communications*,
410 **5**(Supplement C), 19 – 25.
- 411 Kremling, A., Geiselman, J., Ropers, D., & de Jong, H. 2015. Understanding carbon catabolite repres-
412 sion in *Escherichia coli* using quantitative models. *Trends in Microbiology*, **23**(2), 99 – 109.
- 413 Lambert, G., & Kussell, E. 2014. Memory and Fitness Optimization of Bacteria under Fluctuating
414 Environments. *PLOS Genetics*, **10**(9), 1–10.
- 415 Magasanik, B. 1961. Catabolite Repression. *Cold Spring Harb Symp Quant Biol*, **26**, 249–256.
- 416 Maggi, F. 2015. *BRTSim version 1; A general-purpose multiphase and multicomponent computational*
417 *solver for biogeochemical reaction-advection-dispersion processes in porous and non-porous media,*
418 *First edition, Research Report R954, The University of Sydney, Australia, pp 29.*
- 419 Maggi, F., & Riley, W.J. 2010. Mathematical treatment of isotopologue and isotopomer speciation and
420 fractionation in biochemical kinetics. *Geochimica et Cosmochimica Acta*, **74**, 1823–1835.
- 421 Maggi, F., Tang, F.H.M., & Riley, W.J. 2018. The thermodynamic links between substrate, enzyme, and
422 microbial dynamics in MichaelisMentenMonod kinetics. *International Journal of Chemical Kinetics*,
423 1–14.
- 424 Monod, J. 1942. *Recherches sur la croissance des cultures bacteriennes*. Thesis, Hermann et Cie, Paris.
- 425 Monod, J. 1949. The Growth of Bacterial Cultures. *Annual Review of Microbiology*, **3**, 371–394.

- 426 Mukherjee, A., & Ghosh, S. 1987. Regulation of fructose uptake and catabolism by succinate in *Azospir-*
427 *illum brasilense*. *Journal of Bacteriology*, **169**, 4361–4367.
- 428 Nielsen, J., & Villadsen, J. 1992. Modelling of microbial kinetics. *Chemical Engineering Science*, **47**,
429 4225–4270.
- 430 Prommer, H., Barry, D., Chiang, W., & Zheng, C. 2001. PHT3D - A MODFLOW / MT3DMS-based
431 reactive multi-component transport model. *Ground Water*, 477–483.
- 432 Riley, W. J., Maggi, F., Kleber, M., Torn, M. S., Tang, J. Y., Dwivedi, D., & Guerry, N. 2014. Long
433 residence times of rapidly decomposable soil organic matter: application of a multi-phase, multi-
434 component, and vertically resolved model (BAMS1) to soil carbon dynamics. *Geoscientific Model*
435 *Development*, **7**(4), 1335–1355.
- 436 Roca, C., & Olsson, L. 2001. Dynamic responses of *Pseudomonas fluorescens* DF57 to nitrogen or
437 carbon source addition. *Journal of Biotechnology*, **86**(1), 39 – 50.
- 438 Salem, S., Moussa, M.S., & van Loosdrecht, M.C.M. 2006. Determination of the decay rate of nitrifying
439 bacteria. *Biotechnology and Bioengineering*, **94**(2), 252–262.
- 440 Santos-Beneit, F. 2015. The Pho regulon: a huge regulatory network in bacteria. *Frontiers in Microbiol-*
441 *ogy*, **6**, 402–415.
- 442 Schimel, J., Becerra, C.N., & Blankinship, J. 2017. Estimating decay dynamics for enzyme activities in
443 soils from different ecosystems. *Soil Biology and Biochemistry*, **114**, 5 – 11.
- 444 Schimel, J.P., & Weintraub, M.N. 2003. The implications of exoenzyme activity on microbial carbon
445 and nitrogen limitation in soil: a theoretical model. *Soil Biol. Biochem.*, **35**, 549563.
- 446 Stock, J.B., & Zhang, S. 2012. The Biochemistry of Memory. *Current Biology*, **23**(17), 741745.
- 447 Stülke, J., & Hillen, W. 1999. Carbon catabolite repression in bacteria. *Current Opinion in Microbiology*,
448 **2**(2), 195 – 201.
- 449 Taga, M.E., & Bassler, B.L. 2003. Chemical communication among bacteria. *Proceedings of the Na-*
450 *tional Academy of Sciences*, **100**, 14549–14554.
- 451 VanDedem, G., & Moo-Young, M. 1975. A Model for Diauxic Growth. *Biotechnology and Bioengi-*
452 *neering*, **17**, 1301–1312.
- 453 von Bodman, S.B., Willey, J.M., & Diggle, S.P. 2008. Cell-Cell Communication in Bacteria: United We
454 Stand. *Journal of Bacteriology*, **190**, 4377–4391.

- 455 Wang, J., Atolia, E., Hua, B., Savir, Y., Escalante-Chong, R., & Springer, M. 2015. Natural Variation in
456 Preparation for Nutrient Depletion Reveals a CostBenefit Tradeoff. *PLOS Biology*, **13**(1), 1–31.
- 457 Wanner, B. L. 1993. Gene regulation by phosphate in enteric bacteria. *Journal of Cellular Biochemistry*,
458 **51**(1), 47–54.
- 459 Wardle, David A., Bardgett, Richard D., Klironomos, John N., Setälä, Heikki, van der Putten, Wim H., &
460 Wall, Diana H. 2004. Ecological Linkages Between Aboveground and Belowground Biota. *Science*,
461 **304**(5677), 1629–1633.
- 462 Wutzler, T., & Reichstein, M. 2013. Priming and substrate quality interactions in soil organic matter
463 models. *Biogeosciences*, **10**(3), 2089–2103.
- 464 Xu, T., Spycher, N., Sonnenthal, E., Zhang, G., Zheng, L., & Pruess, K. 2011. TOUGHREACT Version
465 2.0: A simulator for subsurface reactive transport under non-isothermal multiphase flow conditions.
466 *Ground Water*, **6**, 763–774.
- 467 Yu, C., & Zheng, C. 2010. HYDRUS: software for flow and transport modeling in variably saturated
468 media. *Ground Water*, **6**, 787–791.
- 469 Zhalnina, K., Louie, K.B., Hao, Z., Mansoori, N., da Rocha, U.N., Shi, S., Cho, H., Karaoz, U., Loqu,
470 D., Bowen, B.P., Firestone, M.K., Northen, T.R., & Brodie, E.L. 2018. Dynamic root exudate chem-
471 istry and microbial substrate preferences drive patterns in rhizosphere microbial community assembly.
472 *Nature Microbiology*, **3**, 470–480.

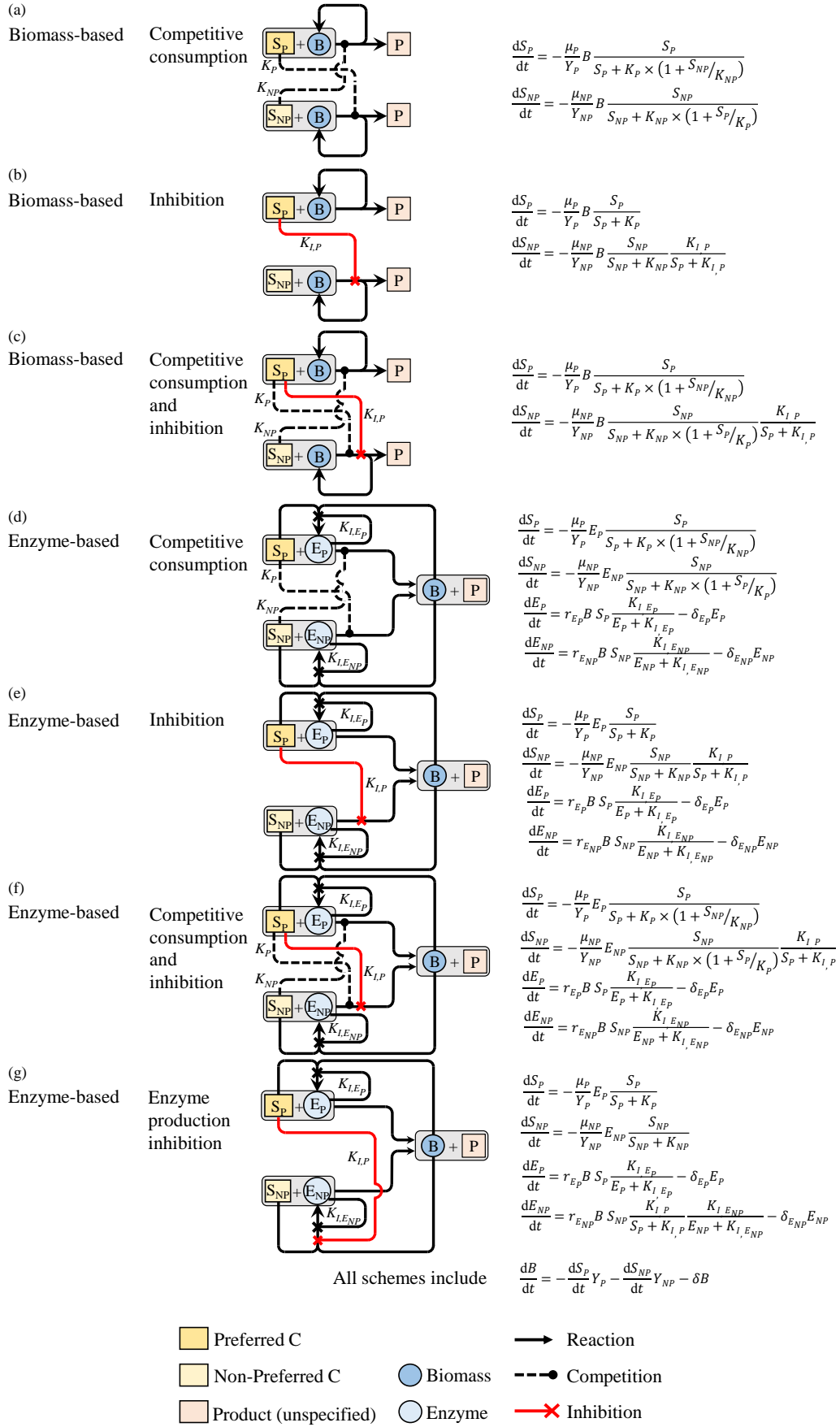


Figure 1: Graphical representation and mathematical description of biomass- and enzyme-based MMM kinetics: (a) Substrate competitive consumption; (b) Non-competitive inhibition of non-preferred C source by preferred C source; (c) Substrate competitive consumption and non-competitive inhibition of non-preferred C source by preferred C source; (d) Substrate competitive consumption; (e) Non-competitive inhibition of non-preferred C source by preferred C source; (f) Substrate competitive consumption and non-competitive inhibition of non-preferred C source by preferred C source; (g) Enzyme production inhibition by preferred C source. Enzyme production was under negative feedback regulation by enzyme concentration.

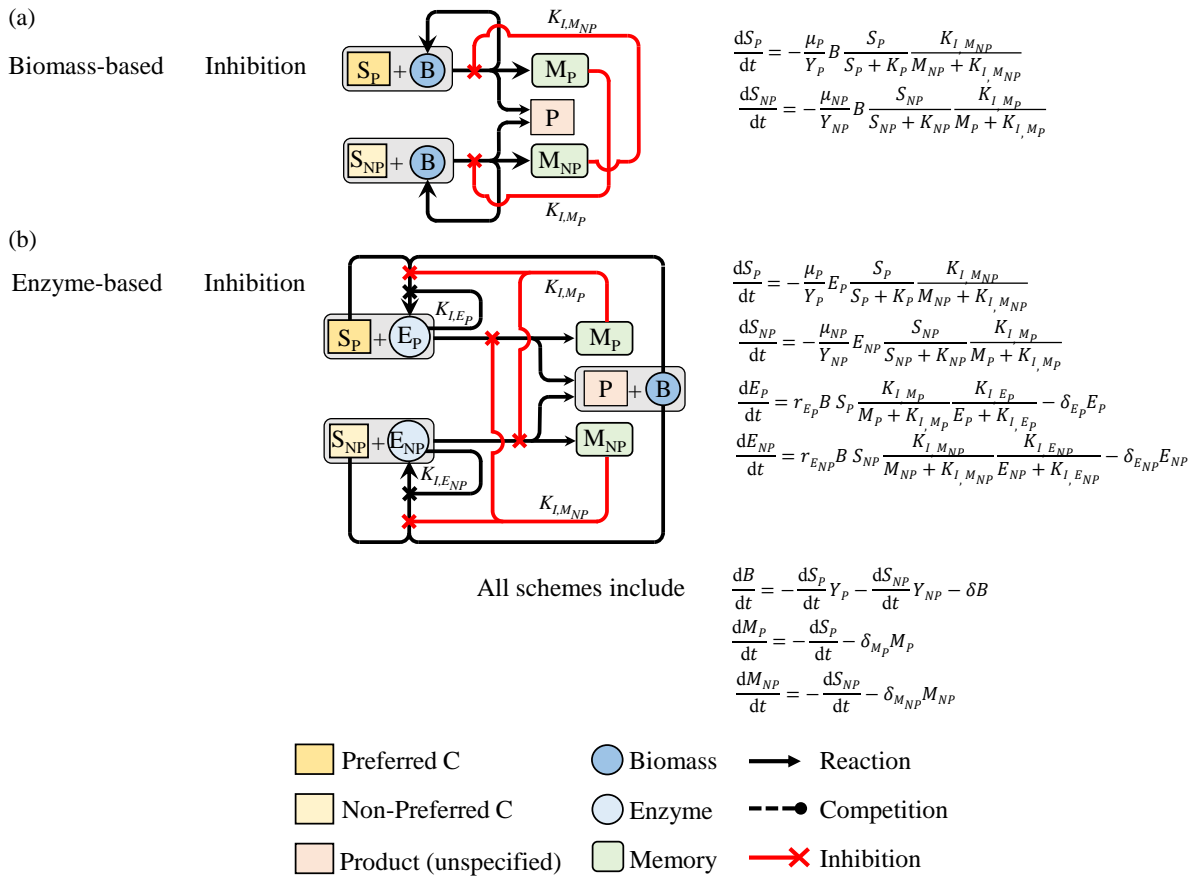


Figure 2: Graphical representation and mathematical description of MACR-C kinetics. (a) Biomass-based and (b) enzyme-based substrate non-competitive inhibition by antagonist memory. Enzyme production was under negative feedback regulation by enzyme concentration and on byproducts formation.

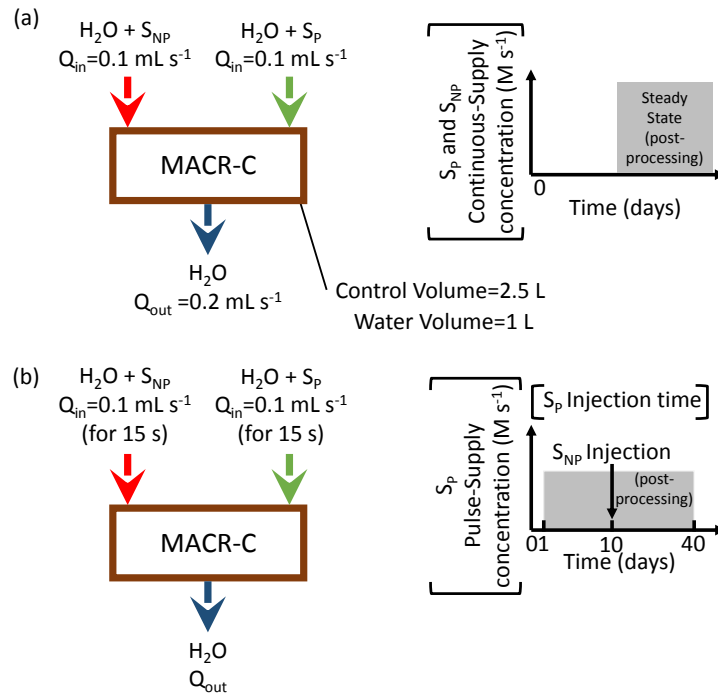


Figure 3: Model scheme for (a) continuous S_P and S_{NP} amendments and (b) single pulse of S_P and S_{NP} . The manipulated variables are enclosed within brackets.

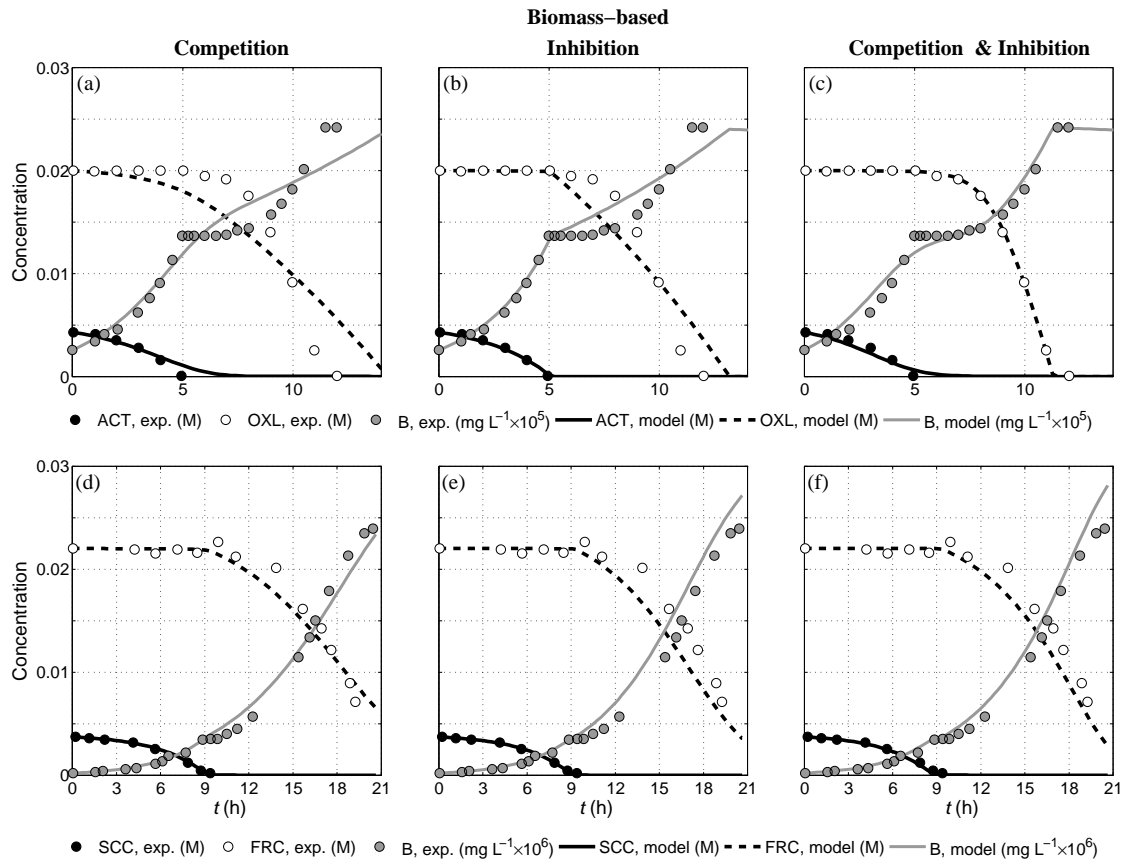


Figure 4: Biomass-based kinetics. ACT-OXL and SCC-FRC consumption with the inoculum pregrown with the preferred C source ACT and SCC, respectively. (a) and (d) Substrate competitive consumption corresponding to the scheme in Figure 1a; (b) and (e) Substrate non-competitive inhibition corresponding to the scheme in Figure 1b; (c) and (f) Substrate competitive consumption and non-competitive inhibition corresponding to the scheme in Figure 1c. Estimated parameters are in Table 1.

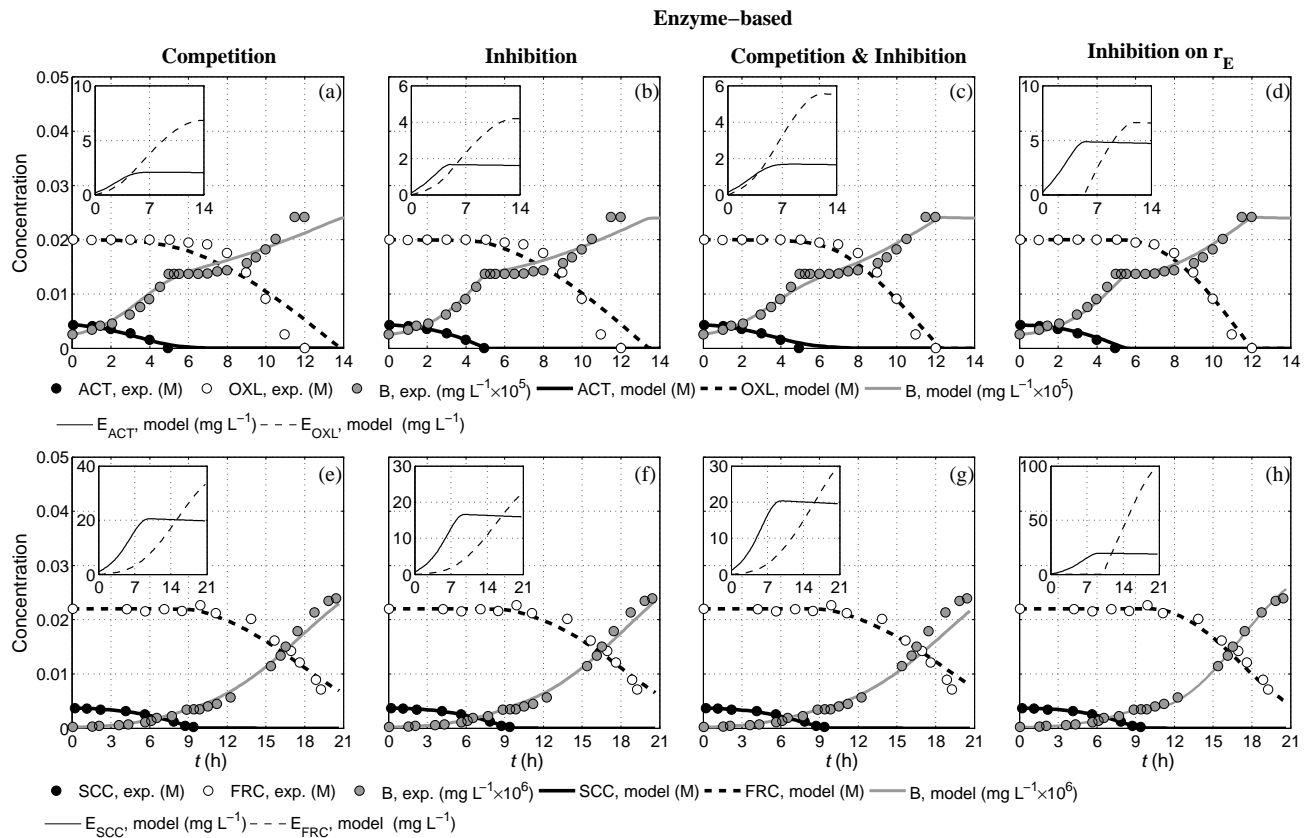


Figure 5: Enzyme-based kinetics. ACT-OXL and SCC-FRC consumption with the inoculum pregrown with the preferred C source ACT and SCC, respectively. (a) and (e) Substrate competitive consumption corresponding to the scheme in Figure 1d; (b) and (f) Substrate non-competitive inhibition corresponding to the scheme in Figure 1e; (c) and (g) Substrate competitive consumption and non-competitive inhibition corresponding to the scheme in Figure 1f; (d) and (h) Substrate inhibition term on enzyme production corresponding to the scheme in Figure 1g. Estimated parameters are in Table 1. Insets in the top right corners show enzyme dynamics.

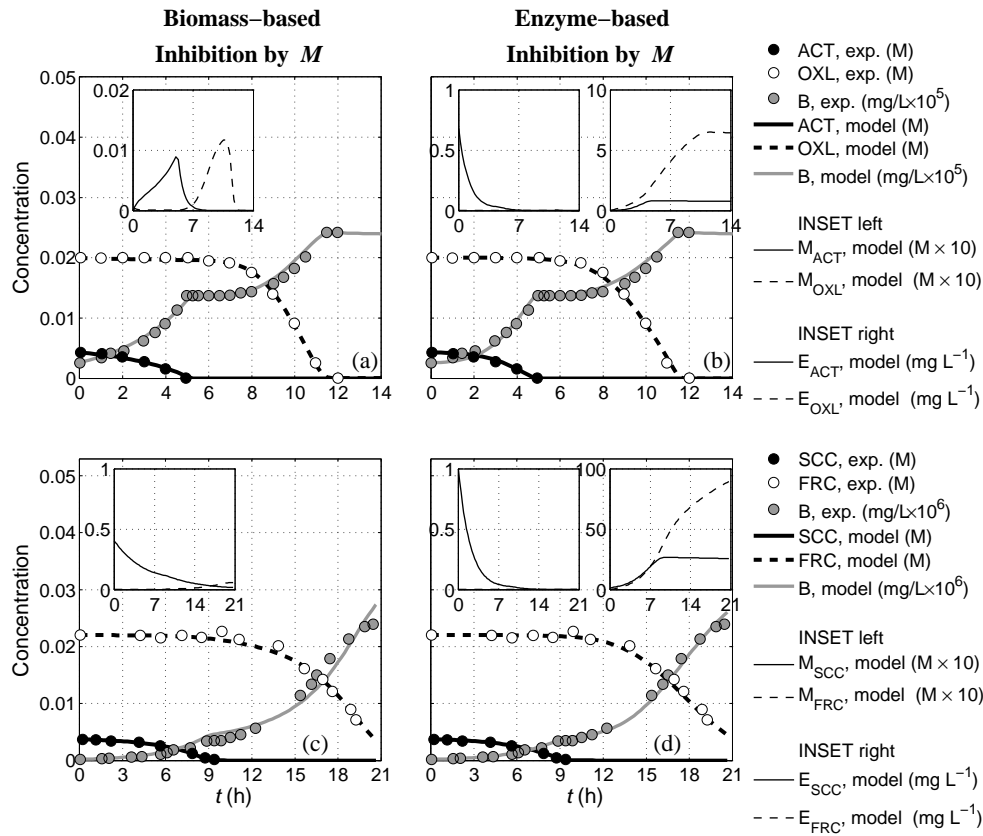


Figure 6: MACR-C kinetics on ACT-OXL and SCC-FRC consumption with the inoculum pregrown with the preferred C source ACT and SCC, respectively. (a) and (c) Memory inhibition to biomass-based substrate consumption corresponding to the scheme in Figure 2a; (b) and (d) Memory inhibition to enzyme-based substrate catalysis corresponding to the scheme in Figure 2b. Estimated parameters are in Table 1. Insets in the top left and right corners show memory and enzyme dynamics, respectively.

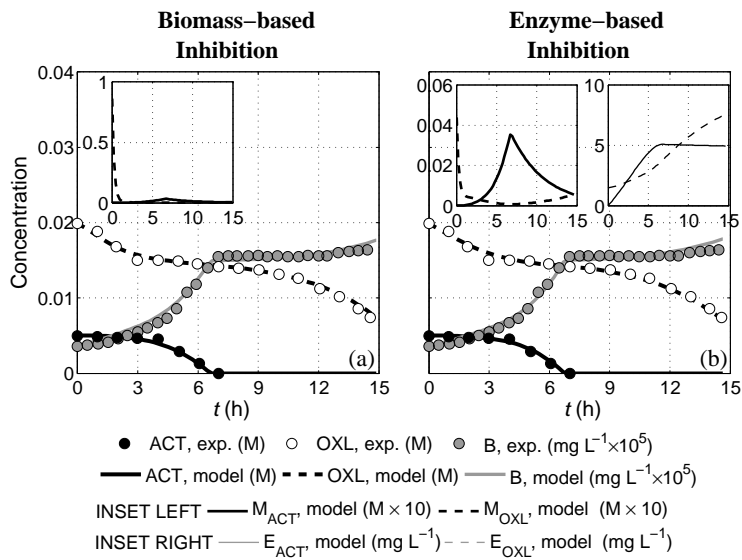


Figure 7: MACR-C kinetics on ACT-OXL consumption with the inoculum pregrown with the non-preferred C-source OXL. (a) Memory inhibition to biomass-based substrate consumption corresponding to the scheme in Figure 2a; (b) Memory inhibition to enzyme-based substrate catalysis corresponding to the scheme in Figure 2b. Estimated parameters are in Table 1.

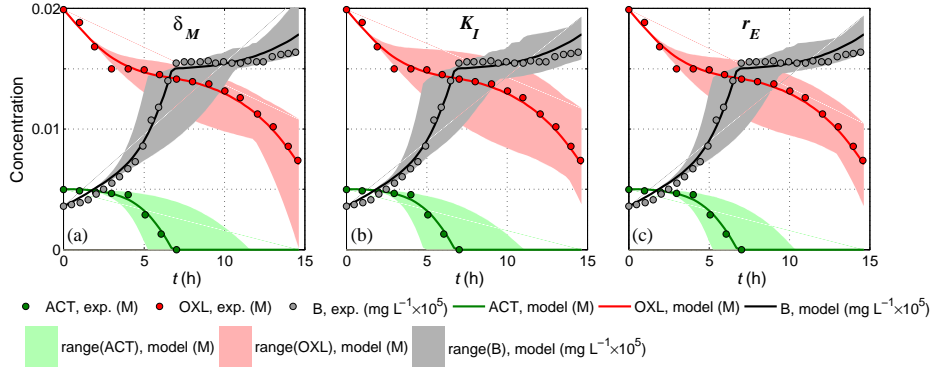


Figure 8: Stochastic sensitivity analysis for enzyme-based MACR-C kinetics. Effect on substrate consumption due to variability of: (a) memory signal degradation rate δ_M ; (b) memory signal inhibition constant $K_{I,M}$; (c) enzyme production rate r_E . Colored areas show the range of predicted substrate concentrations in 1000 simulations.

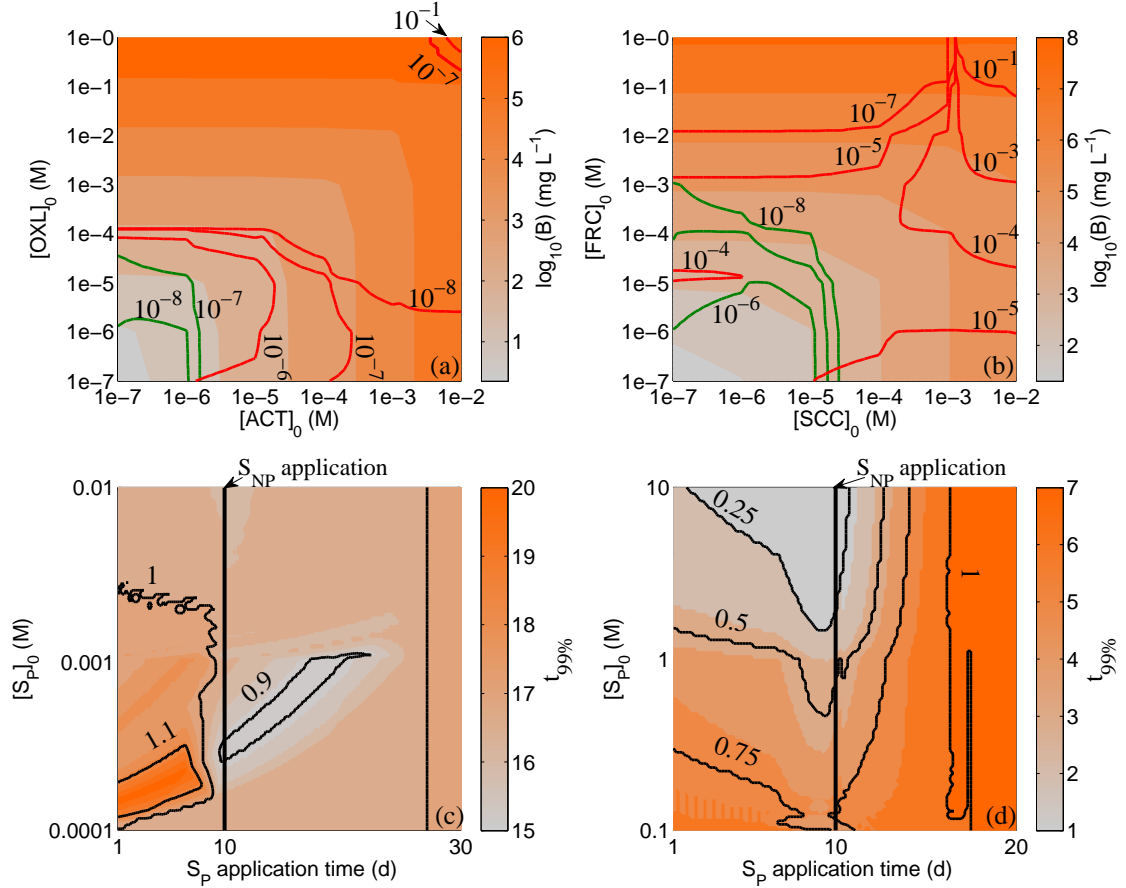


Figure 9: Biomass and substrates concentrations at steady-state as a function of substrates' release concentration at 0.1 mL s^{-1} flow rate: (a) ACT and OXL carbon-source system; (b) SCC and FRC carbon-source system. Green and red contour lines represent the preferred substrate concentration and non-preferred substrate concentration, respectively, in the control volume. Non-preferred substrate consumption time as a function of preferred substrate application time at varying concentrations: (c) ACT (S_p) and OXL (S_{NP} at 0.001 M) carbon-source system; (d) SCC (S_p) and FRC (S_{NP} at 1 M) carbon-source system. Pulses lasted 15 s at 0.1 mL s^{-1} flow rate. Thick black vertical line indicates S_{NP} amendment at day 10. Black contour lines represent the ratio between $t_{99\%}$ in the presence of S_p over $t_{99\%}$ without S_p .

1	2	3	4	5	6	7	8	9	10	11	12	13
Scheme	SubS	pregrowth	μ s ⁻¹	K mol L ⁻¹	K_I mol L ⁻¹	Y_{wet} mg-wet-Bio mol-Subs ⁻¹	Y_{dry} g-C-Bio g-C-Subs ⁻¹	δ_M s ⁻¹	r_E L mol ⁻¹ s ⁻¹	K_{JM} mg L ⁻¹	R ²	NRMSE
Biomass-based, Competition Scheme in Figure 1a Result in Figure 4a	ACT	ACT	1.67×10 ⁻⁴	2.60×10 ⁻⁶		2.59×10 ⁺⁵	5.39×10 ⁻¹				0.97	10.86
	OXL B		1.66×10 ⁻⁵	1.61×10 ⁻⁵		5.50×10 ⁺⁴	1.15×10 ⁻¹				0.97	14.27
Biomass-based, Competition Scheme in Figure 1a Result in Figure 4d	SCC	SCC	9.13×10 ⁻⁵	7.07×10 ⁻⁵		9.39×10 ⁺⁵	9.78×10 ⁻¹				0.99	2.28
	FRC B		1.35×10 ⁻⁴	2.96×10 ⁻²		1.31×10 ⁺⁶	9.07×10 ⁻¹				0.99	6.91
Biomass-based, Inhibition Scheme in Figure 1b Result in Figure 4b	ACT	ACT	9.22×10 ⁻⁵	2.60×10 ⁻⁶		2.59×10 ⁺⁵	5.39×10 ⁻¹				0.99	3.53
	OXL B		2.05×10 ⁻⁵	1.61×10 ⁻⁵	3.71×10 ⁻⁵	5.50×10 ⁺⁴	1.15×10 ⁻¹				0.99	10.59
Biomass-based, Inhibition Scheme in Figure 1b Result in Figure 4e	SCC	SCC	9.23×10 ⁻⁵	7.07×10 ⁻⁵		9.39×10 ⁺⁵	9.78×10 ⁻¹				0.99	2.39
	FRC B		1.45×10 ⁻⁴	2.50×10 ⁻²	1.05×10 ⁻⁵	1.31×10 ⁺⁶	9.07×10 ⁻¹				0.99	12.93
Biomass-based, Competition & Inhibition Scheme in Figure 1c Result in Figure 4c	ACT	ACT	2.07×10 ⁻⁴	2.60×10 ⁻⁶		2.59×10 ⁺⁵	5.39×10 ⁻¹				0.95	9.56
	OXL B		4.92×10 ⁻⁵	1.61×10 ⁻⁵	1.78×10 ⁻⁵	5.50×10 ⁺⁴	1.15×10 ⁻¹				0.95	0.70
Biomass-based, Competition & Inhibition Scheme in Figure 1c Result in Figure 4f	SCC	SCC	9.84×10 ⁻⁵	7.07×10 ⁻⁵		9.39×10 ⁺⁵	9.78×10 ⁻¹				0.99	4.52
	FRC B		8.36×10 ⁻⁵	2.09×10 ⁻²	1.82×10 ⁻⁶	1.31×10 ⁺⁶	9.07×10 ⁻¹				0.99	10.29
Biomass-based, MACR-C Scheme in Figure 2a Result in Figure 6a	ACT	ACT	8.87×10 ⁻⁵	2.60×10 ⁻⁶	2.79×10 ⁻¹	2.59×10 ⁺⁵	5.39×10 ⁻¹	4.14×10 ⁻⁴			0.99	4.23
	OXL B		5.85×10 ⁻⁵	1.06×10 ⁻⁵	1.06×10 ⁻⁵	5.50×10 ⁺⁴	1.15×10 ⁻¹	1.57×10 ⁻³			0.99	1.07
Biomass-based, MACR-C Scheme in Figure 2a Result in Figure 6c	SCC	SCC	8.67×10 ⁻⁵	7.07×10 ⁻⁵	3.52×10 ⁻¹	9.39×10 ⁺⁵	9.78×10 ⁻¹	4.62×10 ⁻⁵			0.99	2.81
	FRC B		8.18×10 ⁻⁴	2.23×10 ⁻²	7.03×10 ⁻⁴	1.31×10 ⁺⁶	9.07×10 ⁻¹	1.25×10 ⁻⁴			0.99	4.09
Biomass-based, MACR-C Scheme in Figure 2a Result in Figure 7a	ACT	ACT	1.84×10 ⁻⁴	2.67×10 ⁻⁶	5.36×10 ⁻⁵	1.80×10 ⁺⁵	3.75×10 ⁻¹	7.71×10 ⁻⁵			0.99	4.66
	OXL B	OXL	8.07×10 ⁻⁵	1.62×10 ⁻⁵	8.12×10 ⁻⁵	4.58×10 ⁺⁴	9.55×10 ⁻²	1.01×10 ⁻³			0.99	2.71
Enzyme-based, Competition Scheme in Figure 1d Result in 5a	ACT	ACT	5.07×10 ⁺¹	2.60×10 ⁻⁶		2.59×10 ⁺⁵	5.39×10 ⁻¹	6.98×10 ⁻⁵			0.97	7.20
	OXL B		1.18×10 ⁺¹	1.61×10 ⁻⁵		5.50×10 ⁺⁴	1.15×10 ⁻¹	9.86×10 ⁻⁶			0.97	12.37
Enzyme-based, Competition Scheme in Figure 1d Result in 5e	SCC	SCC	1.19×10 ⁺⁰	7.07×10 ⁻⁵		9.39×10 ⁺⁵	9.78×10 ⁻¹	3.75×10 ⁻⁴			0.99	1.83
	FRC B		4.59×10 ⁺⁰	1.89×10 ⁻²		1.31×10 ⁺⁶	9.07×10 ⁻¹	7.76×10 ⁻⁶			0.99	7.01
Enzyme-based, Inhibition Scheme in Figure 1e Result in 5b	ACT	ACT	2.59×10 ⁺¹	2.60×10 ⁻⁶		2.59×10 ⁺⁵	5.39×10 ⁻¹	6.51×10 ⁻⁵			0.99	1.17
	OXL B		2.06×10 ⁺¹	1.61×10 ⁻⁵	6.10×10 ⁻⁴	5.50×10 ⁺⁴	1.15×10 ⁻¹	5.89×10 ⁻⁶			0.99	10.86
Enzyme-based, Inhibition Scheme in Figure 1e Result in 5f	SCC	SCC	1.44×10 ⁺⁰	7.07×10 ⁻⁵		9.39×10 ⁺⁵	9.78×10 ⁻¹	2.90×10 ⁻⁴			0.99	1.75
	FRC B		5.61×10 ⁺⁰	1.17×10 ⁻²	2.15×10 ⁻⁴	1.31×10 ⁺⁶	9.07×10 ⁻¹	4.49×10 ⁻⁶			0.99	6.61
Enzyme-based, Competition & Inhibition Scheme in Figure 1f Result in 5c	ACT	ACT	5.66×10 ⁺¹	2.60×10 ⁻⁶		2.59×10 ⁺⁵	5.39×10 ⁻¹	5.13×10 ⁻⁵			0.98	9.40
	OXL B		2.07×10 ⁺¹	1.61×10 ⁻⁵	5.09×10 ⁻⁴	5.50×10 ⁺⁴	1.15×10 ⁻¹	8.87×10 ⁻⁶			0.98	5.65
Enzyme-based, Competition & Inhibition Scheme in Figure 1f Result in 5g	SCC	SCC	1.24×10 ⁺⁰	7.07×10 ⁻⁵		9.39×10 ⁺⁵	9.78×10 ⁻¹	3.78×10 ⁻⁴			0.99	3.10
	FRC B		3.57×10 ⁺⁰	1.11×10 ⁻²	3.73×10 ⁻⁴	1.31×10 ⁺⁶	9.07×10 ⁻¹	6.73×10 ⁻⁶			0.99	7.73
Enzyme-based, r_E Inhibition Scheme in Figure 1g Result in 5d	ACT	ACT	8.20×10 ⁺⁰	2.60×10 ⁻⁶		2.59×10 ⁺⁵	5.39×10 ⁻¹	1.93×10 ⁻⁴			0.99	8.16
	OXL B		2.04×10 ⁺¹	1.61×10 ⁻⁵		5.50×10 ⁺⁴	1.15×10 ⁻¹	1.60×10 ⁻⁵	2.96×10 ⁻⁵		0.99	3.98
Enzyme-based, r_E Inhibition Scheme in Figure 1g Result in 5h	SCC	SCC	1.27×10 ⁺⁰	7.07×10 ⁻⁵		9.39×10 ⁺⁵	9.78×10 ⁻¹	3.90×10 ⁻⁴			0.99	2.31
	FRC B		2.26×10 ⁺⁰	2.00×10 ⁻²		1.31×10 ⁺⁶	9.07×10 ⁻¹	5.57×10 ⁻⁵	6.69×10 ⁻⁰		0.99	5.44
Enzyme-based, MACR-C Scheme in Figure 2b Result in 6a	ACT	ACT	1.14×10 ⁺²	2.60×10 ⁻⁶	8.82×10 ⁻⁶	2.59×10 ⁺⁵	5.39×10 ⁻¹	2.33×10 ⁻⁴	1.18×10 ⁻⁴	3.70×10 ⁻³	0.99	4.16
	OXL B		2.76×10 ⁺¹	1.61×10 ⁻⁵	2.14×10 ⁻⁴	5.50×10 ⁺⁴	1.15×10 ⁻¹	4.59×10 ⁻³	1.11×10 ⁻⁵	1.91×10 ⁻³	0.99	1.93
Enzyme-based, MACR-C Scheme in Figure 2b Result in 6c	SCC	SCC	9.85×10 ⁻¹	7.07×10 ⁻⁵	3.26×10 ⁻¹	9.39×10 ⁺⁵	9.78×10 ⁻¹	1.34×10 ⁻⁴	3.91×10 ⁻⁴	1.50×10 ⁻¹	0.99	2.09
	FRC B		3.10×10 ⁺⁰	2.00×10 ⁻¹	1.61×10 ⁻⁴	1.31×10 ⁺⁶	9.07×10 ⁻¹	3.81×10 ⁻³	5.05×10 ⁻⁵	2.70×10 ⁻⁵	0.99	4.00
Enzyme-based, MACR-C Scheme in Figure 2b Result in 7b	ACT	ACT	1.14×10 ⁺²	2.60×10 ⁻⁶	8.82×10 ⁻⁶	1.80×10 ⁺⁵	3.75×10 ⁻¹	6.59×10 ⁻⁵	1.18×10 ⁻⁴	3.70×10 ⁻³	0.99	4.20
	OXL B	OXL	2.76×10 ⁺¹	1.61×10 ⁻⁵	2.14×10 ⁻⁴	4.58×10 ⁺⁴	9.55×10 ⁻²	9.93×10 ⁻⁴	1.11×10 ⁻⁵	1.91×10 ⁻³	0.99	2.65

Table 1: Estimated kinetic parameters for ACT and OXL metabolism using the schemes in Figures 1 and 2. Calibration curves against observations are plotted in Figures 4, 5, 6, and 7. Tabulated goodness-of-fit are against experiments from Dijkhuizen *et al.* (1980) and Mukherjee & Ghosh (1987). Diauxic growth of *Pseudomonas oxalaticus* on ACT and OXL was conducted in aerobic conditions, pH 7.5, and $T = 30^\circ$; estimated initial biomass concentration was 256 mg-wet-Bio L⁻¹ and 360 mg-wet-Bio L⁻¹ when the inoculum was pregrown in ACT and OXL, respectively. Diauxic growth of *Azospirillum brasilense* on SCC and FRC was conducted in aerobic conditions, pH 7.6, and $T = 32^\circ$; initial biomass concentration was 205 mg-wet-Bio L⁻¹ with the inoculum pregrown in SCC.